

FRB 171019: an event of binary neutron star merger?

Jin-Chen Jiang (姜金辰)^{1,2}, Wei-Yang Wang (王维扬)^{3,4}, Rui Luo (罗睿)⁵, Shuang Du (杜双)¹,
Xuele Chen (陈学雷)³, Ke-Jia Lee (李柯伽)^{1,6} and Ren-Xin Xu (徐仁新)^{1,6}

¹ State Key Laboratory of Nuclear Physics and Technology, School of Physics, Peking University, Beijing 100871, China; jiangjinchen@pku.edu.cn

² National Astronomical Observatories, Chinese Academy of Sciences, Beijing 100101, China

³ Key Laboratory of Computational Astrophysics, National Astronomical Observatories, Chinese Academy of Sciences, Beijing 100101, China

⁴ School of Astronomy and Space Sciences, University of Chinese Academy of Sciences, Beijing 100049, China

⁵ CSIRO Astronomy and Space Science, ATNF, Box 76 Epping, NSW 1710, Australia

⁶ Kavli Institute for Astronomy and Astrophysics, Peking University, Beijing 100871, China

Received 2019 October 3; accepted 2019 December 12

Abstract The fast radio burst, FRB 171019, was relatively bright when discovered first by ASKAP but was identified as a repeater with three faint bursts detected later by GBT and CHIME. These observations lead to the discussion of whether the first bright burst shares the same mechanism with the following repeating bursts. A model of binary neutron star merger is proposed for FRB 171019, in which the first bright burst occurred during the merger event, while the subsequent repeating bursts are starquake-induced, and generally fainter, as the energy release rate for the starquakes can hardly exceed that of the catastrophic merger event. This scenario is consistent with the observation that no later burst detected is as bright as the first one.

Key words: pulsars: general — stars: neutron — dense matter — gravitational waves

1 INTRODUCTION

Fast radio bursts (FRBs), which are millisecond extragalactic radio flashes, still have mysteries on their cosmological origins (Lorimer et al. 2007; Keane et al. 2012; Thornton et al. 2013; Kulkarni et al. 2014; Petroff et al. 2015, 2016; Chatterjee et al. 2017). Until now, dozens of FRBs have been identified as repeaters (Spitler et al. 2016; CHIME/FRB Collaboration et al. 2019a,b).

A very interesting open question is whether all FRBs repeat. There are a lot of efforts having been made to study the relationship between FRB repeaters and non-repeating FRBs. The first repeater, FRB 121102, was localized in a low-metallicity starforming dwarf galaxy ($\sim 10^8 M_{\odot}$) at a redshift of $z = 0.193$ (Chatterjee et al. 2017; Marcote et al. 2017; Tendulkar et al. 2017) with an extremely magneto ionic environment (Michilli et al. 2018), which directly confirmed the cosmological origin. However, recently, a single FRB which has not been observed repeating, was localized in a more massive spiral galaxy (Bannister et al.

2019), in contrast to the host galaxy of FRB 121102. The differences of their host galaxy lead to the discussion of multi-origins between repeaters and non-repeating FRBs.

Repeaters also exhibit some different properties to non-repeating FRBs. For instance, the time–frequency downward drifting pattern appears in at least some of repeaters’ sub-pulses (Hessels et al. 2019; CHIME/FRB Collaboration et al. 2019a,b), while non-repeating FRBs lack such structures, which suggests that these are most likely to be a common feature for repeaters (Wang et al. 2019). Additionally, repeating sources tend to show less luminous bursts than most non-repeating FRBs (Luo et al. 2018, 2020). Both may hint that repeating FRBs possibly share different radiative and energy-providing mechanism with non-repeating FRBs.

Motivated by the recent observation of FRB 171019, which was reported to exhibit repeating bursts ~ 590 times fainter than its discovery burst (Kumar et al. 2019), we propose an FRB engine of merging normal neutron star (NS) or strangeon star (SS, see Xu 2018 for a brief introduc-

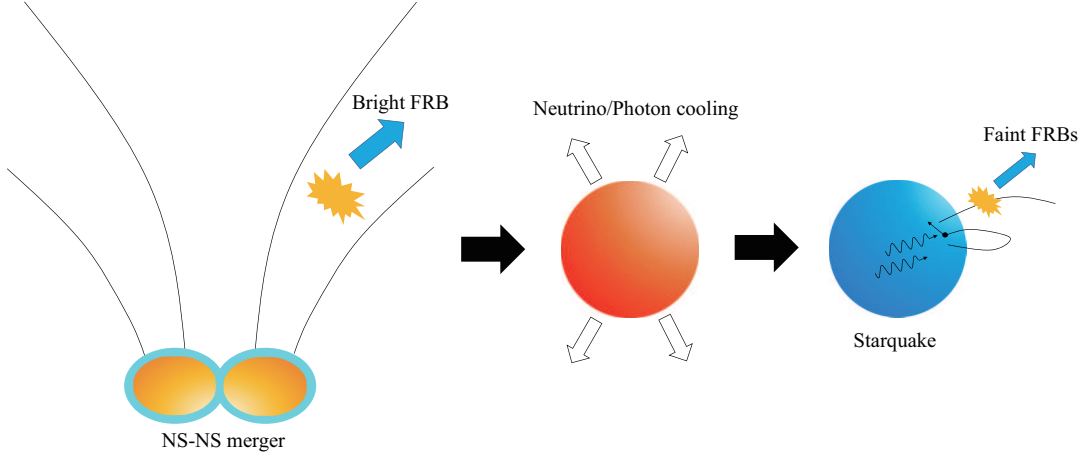


Fig. 1 Schematic diagram of the model. The first discovered bright FRB is supported by fast orbital energy release during the two NS merger. After that, a post-merger of long-lived neutron stars forms and cools rapidly because of the neutrino/photon cooling. Starquakes would occur after the stellar solidification. The magnetic line footpoint oscillation may re-activate magnetospheric e^\pm -pair production or even trigger magnetic reconnection, which accelerates charged bunches emitting the following faint FRBs.

tion) to power both non-repeating catastrophic and repeating bursts (see Fig. 1). In fact, several catastrophic events, which can generate new-born pulsar-like compact stars, have already been involved in interpreting non-repeating bright FRBs (e.g., Jin et al. 2018; Kashiyama et al. 2013; Totani 2013; Wang et al. 2016; Liu 2018). Yamasaki et al. (2018) speculated that the remnant pulsar after the merger event could reproduce periodically repeating FRBs. The following repeating FRBs could be caused by the stellar rigidity-induced starquakes (Wang et al. 2018b; Suvorov & Kokkotas 2019) on the remnant compact star (either normal neutron star or stangeon star). The model is introduced in Section 2, and its applications to FRB 171019 are discussed in Section 3. A summary and discussion are given in Section 4.

2 THE MODEL

2.1 Non-repeating FRB Generated by NS-NS or SS-SS Merger

From the observations of many non-repeating FRBs, one can estimate the luminosity

$$L = 4\pi D^2 \frac{\delta\Omega}{4\pi} S_\nu \Delta\nu \quad (1)$$

$$\simeq 10^{43} D_{\text{Gpc}}^2 \left(\frac{\delta\Omega}{4\pi}\right) \left(\frac{S_\nu}{10 \text{ Jy}}\right) \Delta\nu_{\text{GHz}} \text{ erg s}^{-1},$$

where D_{Gpc} is the source distance in Gpc, $\delta\Omega$ is the beam angle, S_ν is the flux density and $\Delta\nu_{\text{GHz}}$ is the frequency bandwidth in GHz. Such a bright emission is generally considered to be coherent radiation.

Totani (2013), Wang et al. (2016) and Murase et al. (2017) concluded that FRB emission can occur during the

precursor phase of compact star mergers. In this model, we propose that the one-off FRBs are generated by NS-NS or SS-SS merger. Our model is based on the unipolar inductor model, which was first proposed for the Jupiter-Io system (Goldreich & Lynden-Bell 1969). The event rate of the merger bursts should be equivalent to the NS-NS merger rate, viz. $\sim 10^{-1} - 10^3 \text{ Gpc}^{-3} \text{ yr}^{-1}$ (Chruslinska et al. 2018; Paul 2018; Pol et al. 2019).

The orbital angular velocity can be calculated as $\Omega = (GM(1+q)/a^3)^{0.5} \sim 3.7 \times 10^3 \text{ rad s}^{-1}$, where $q = 1$ is adopted as the mass ratio of the two NSs, $a = 30 \text{ km}$ is adopted as the distance between two NSs and $M = 1.4M_\odot$ adopted as the mass of NS. In the late inspiral of binary coalescence, the dipolar configuration of the magnetic field between two NSs should be severely distorted due to magnetic interaction, while the far field should remain dipolar with a total magnetic moment $\mu_{\text{tot}} = \mu_1 + \mu_2$. Inside the region between the two NSs, charged particles are able to move across the orbital plane in the distorted magnetic field, therefore the magnetosphere around the orbital plane can be treated as a conducting plate. Under the assumption of magnetic moment conservation and a parallel configuration, the surface magnetic field can be estimated as

$$B \sim \frac{\mu_{\text{tot}}}{\pi a^2 R_*} \sim \frac{8}{3} \left(\frac{R_*}{a}\right)^2 B_* \quad (2)$$

$$= 3.0 \times 10^{11} B_{*,12} R_{*,6}^2 a_{6.5}^{-2} \text{ G},$$

where $a \sim 30 \text{ km}$, $R_* \sim 10 \text{ km}$ is the typical pulsar radius, $B_* \sim 10^{12} \text{ G}$ is the typical surface magnetic field on pulsars, and the convention $Q_n = Q/10^n$ in cgs units is adopted.

The orbital evolution of the binary is dominated by gravitational-wave radiation. Therefore, one can estimate the distance evolution as (Peters 1964)

$$a = a_0 \left[1 - \frac{256G^3 M^3 q(1+q)}{5a_0^4 c^5} t \right]^{\frac{1}{4}} \quad (3)$$

$$= 20(1 - 1695t)^{\frac{1}{4}} \text{ km}.$$

We set $a_0 = 20$ km for the case when the surfaces of the two NSs touch with each other. One can then estimate the timescale of ~ 2 ms for the process (from $a = 30$ km to $a_0 = 20$ km for $q = 1$), which is consistent with the FRB duration.

On the conducting plate, the open field line region can be estimated by the proportion of its magnetic flux against the total magnetic flux,

$$r_{\text{cap}} = (a + R_*) \sqrt{\frac{\Phi_{\text{open}}}{\Phi_{\text{tot}}}}$$

$$= (a + R_*) \left(\frac{\int_{R_{\text{lc}}}^{+\infty} \frac{r}{r^3} dr}{\int_{a+R_*}^{+\infty} \frac{r}{r^3} dr} \right)^{\frac{1}{2}} \quad (4)$$

$$= (a + R_*)^{\frac{3}{2}} R_{\text{lc}}^{-\frac{1}{2}},$$

where $R_{\text{lc}} = c/\Omega$ is the radius of light cylinder.

A potential drop produced in the unipolar model is

$$U \simeq \frac{B\Omega r_{\text{cap}}^2}{2c}. \quad (5)$$

This potential can trigger pair-production avalanches that creates charged bunches. The bunches stream outward along open magnetic field lines, generating coherent radio emissions. The charge density in the magnetosphere of a pulsar is given by (Goldreich & Julian 1969)

$$\rho_e \simeq \rho_{\text{GJ}} \simeq \frac{\Omega B}{2\pi c}$$

$$= 5.8 \times 10^3 M_{33.44}^{\frac{1}{2}} R_{*,6}^2 B_{*,12} a_{6.5}^{-\frac{7}{2}} \left(\frac{1+q}{2} \right)^{\frac{1}{2}} \text{ esu}, \quad (6)$$

where ρ_{GJ} is the Goldreich–Julian density, B is the magnetic field. The energy releasing rate of the magnetosphere during merger is given by

$$\dot{E} \simeq U\pi r_{\text{cap}}^2 \rho_e c$$

$$\simeq \frac{16}{9c^3} B_*^2 G^2 M^2 (1+q)^2 \left(\frac{R_*}{a} \right)^4 \left(1 + \frac{R_*}{a} \right)^6$$

$$= 6.3 \times 10^{44} B_{*,12}^2 M_{33.44}^2$$

$$\times \left(\frac{1+q}{2} \right)^2 \left(\frac{R_{*,6}}{a_{6.5}} \right)^4 \left(1 + \frac{R_{*,6}}{a_{6.5}} \right)^6 \text{ erg s}^{-1}. \quad (7)$$

If radio efficiency is $\sim 10^{-3}$ and the beaming factor is 10^2 , then the isotropic luminosity matches the typical luminosity of non-repeating FRBs, $L_{\text{iso}} \sim 10^{-3} \times 10^2 \times \dot{E} \sim 10^{43} \text{ erg s}^{-1}$.

This calculation assumed the magnetic moments of the two merger stars are both parallel to the normal direction of the orbital plane (usually denoted as the ‘‘U/U case’’), which should result in the largest \dot{E} . The above result is consistent with the \dot{E} of the U/U case in Palenzuela et al. 2013; Ponce et al. 2014; Wang et al. 2018a. For oblique configurations, the total magnetic moment $|\mu_{\text{tot}}| = |\mu_1 + \mu_2| < |\mu_1| + |\mu_2|$. The antiparallel configuration results in the smallest $|\mu_{\text{tot}}| = |\mu_1 - \mu_2|$, which can be smaller than μ_1 and μ_2 by several orders of magnitudes.

The compact star mergers may also produce other observable effects. The detection of GRB 170817A corresponding to GW 170817 (Abbott et al. 2017) indicates that short γ -ray bursts can be generated by compact star mergers. Therefore, our model infers that a short GRB may be generated as the counterpart of a one-off FRB, which is consistent with the γ -ray counterpart to FRB 131104 (DeLaunay et al. 2016).

2.2 Subsequent Repeating FRBs Generated by Starquakes

We predict a new-born pulsar-like compact star left after a fraction of NS-NS or SS-SS merger. We suggest that the remnant object should live for at least several years to generate the subsequent repeating FRBs. NS-NS or SS-SS mergers do not always deliver long-lived compact stars. If the remnant mass is larger than the maximum mass for NS or SS, the merger product should be a blackhole. With uniform rotation, the maximum mass of NS or SS can be larger than the Tolman–Oppenheimer–Volkoff (TOV) maximum mass, hence supermassive. A supermassive remnant NS or SS, collapsing years after merger due to the braking of magnetic dipolar radiation or gravitational wave radiation, may also fit in our model. In addition, the geometric factor of the anisotropy further reduce the event rate of such sources. When taking the theoretical approach, the volumetric density of repeating FRB sources is affected by the star formation history, the mass function of NS binaries, the merger dynamics and maximum mass of NS, some of which are still highly uncertain in theories. On the other hand, taking the observational approach, James (2019) limits the volumetric density of repeating FRBs to be $< 70 \text{ Gpc}^{-3}$. Adopting the burst rate of repeating FRB 121102, $5.7_{-2.0}^{+3.0} \text{ day}^{-1}$ (Oppermann et al. 2018), as the burst rate for all repeating FRBs, the observed repeating bursts from such NS-NS remnants should

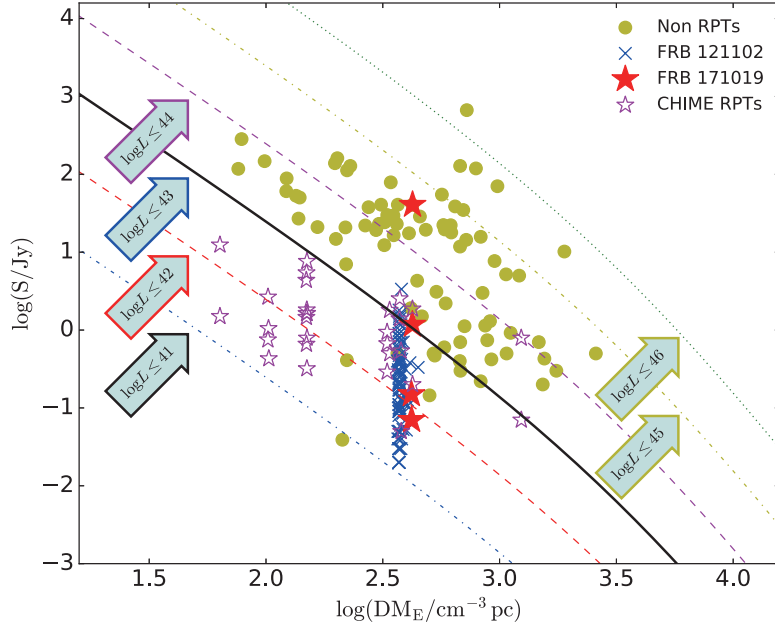


Fig. 2 A radio flux-dispersion measure ($S - DM_E$) diagram for FRBs, with DM_E the dispersion measure deducting the contribution by the Milky Way at the direction. *Dots* represent non-repeating FRBs, *filling pentagrams* represent FRB 171019, *empty pentagrams* represent CHIME repeaters, and *cross marks* represent FRB 121102. The *curves* represent approximately constant radio luminosity.

be $\lesssim 10^5 \text{ Gpc}^{-3} \text{ yr}^{-1}$ for the more sensitive telescopes like GBT and CHIME. In this scenario, it is rather difficult for ASKAP-like small dishes to detect repeating events, which is consistent with the prediction by Yamasaki et al. (2018).

When the initial proto-compact star is formed, gravitational energy would be stored in the compact star as a form of initial thermal energy. Consequently, the temperature of the inner core will be $\sim (30 - 50) \text{ MeV}$. In the first following stage, neutrino emissions make the star becoming cooling very rapidly. However, different equation of states can lead to different cooling behavior.

On the one hand, in the regime of normal neutron star, for a proto-neutron star, it shrinks into $\sim 10 \text{ km}$ within several tens of seconds because of the powerful neutrino-induced cooling down (Pons et al. 1999). The crust has a relatively lower neutrino emissivity than the core. This makes the crust cool more slowly than the core and the surface temperature decreases slowly during the first ten to hundred years (Chamel & Haensel 2008). After that, when the cooling wave from the core reaches the surface, the surface temperature will drop sharply.

On the other hand, the cooling process for a new-born SS consists of three stages (Dai et al. 2011). The first stage is a rapidly cooling process caused by the neutrino and photons emitting at the very beginning. This process spends several tens seconds but in principle faster than the first stage of an NS cooling (Yuan et al. 2017). The SS enters then the second stage, at which the surface temper-

ature remains constant roughly and the liquid SS begins to be solidified, when the temperature drops to the melting point temperature $T_p \sim 0.1 \text{ MeV}$. The time scale of the liquid-solid phase transition can be estimated as

$$t_{\text{solid}} = \frac{E_{\text{in}}}{4\pi R^2 \sigma T_p^4} = 7.8 \times 10^6 E_{\text{in},52} R_6^{-4} \text{ s}, \quad (8)$$

where E_{in} is energy release during the phase transition, σ is the Stefan-Boltzman constant and R is the stellar radius. After the solidification, the newly-born SS will rapidly release its residual inner energy because of its low thermal capacity (Yu & Xu 2011).

Basically, whether it is an NS or an SS, the magnetic field lines are anchored to the stellar surface and their geometry is determined by the motion of the footpoints. For a new-born compact star, there are several kinds of instability which may be driven by gravitational, magnetic or rotational energy. If the instability can grow very fast in the stellar crust, making the pressure exceed a threshold stress, crust quake would happen. Seismic waves, created by the sudden release of energy, diffuse in the crust, which can help some local instabilities growing. The characteristics of self-organized criticality observed in earthquakes, are very expected to be seen in some compact star activities (e.g., Cheng et al. 1996; Duncan 1998; Göğüş et al. 1999). The compact star, which is suggested to be a dead pulsar (i.e., beyond the pulsar death line), can be then excited due to the solid crust quake. A similar but different story of strangeon star was presented in Lin et al. (2015).

In the regime of normal NS, crust shear can trigger the footpoint motion, therefore the magnetic curl or twist are ejected into the magnetosphere from the crust in $\tau \simeq R/v_A \sim 1$ ms (Thompson et al. 2002), where v_A is the Alfvén speed. During this process, charged particles in the magnetosphere, are suddenly accelerated to be ultra-relativistic by the quake-induced magnetic reconnection, and form charged bunches. In general, the cooling timescale for curvature radiation in the observer’s rest frame is much smaller than FRB’s typical duration. Thus, it requires a strong electric field parallel E_{\parallel} to the B-field that can accelerate electrons, supplying the kinetic energy to balance radiation loss, which is given by (Kumar et al. 2017)

$$E_{\parallel} = \frac{\gamma_e mc}{et_{\text{cool}}} = 3 \times 10^8 \nu_9 N_{e,24} \gamma_2^{-2} \text{ esu}, \quad (9)$$

where γ_e is the Lorentz factor of electrons, ν is the emission frequency of curvature radiation, and N_e is the electron number. The E_{\parallel} to the B-field formed by the magnetic reconnection is given by

$$E_{\parallel} \simeq \frac{2\pi\sigma_s v_A B}{c} = 2.1 \times 10^9 \sigma_{s,-3} v_{A,8} B_{14} \text{ esu}, \quad (10)$$

where $\sigma_s = \xi/\lambda$ is the strain, in which ξ is the amplitude of oscillations and λ is the characteristic wavelength of oscillations.

Let us consider the pair production forming charged bunches which emit coherent curvature radiation. Basically, several authors have discussed curvature radiation from charged bunches from pulsar magnetospheres to explain FRBs (e.g., Katz 2014; Kumar et al. 2017; Yang & Zhang 2018). If the charge density prompted by the stellar rotation $\rho_{G,J}$ and local twist is insufficient to screen E_{\parallel} , sparks would occur at the polar gap regions which creates emitting charged bunches (Wadiasingh & Timokhin 2019). The number density due to the footpoint motion can be estimated as

$$n_e \simeq \frac{E_{\parallel}}{4\pi e\lambda} = 3.5 \times 10^{12} \sigma_{s,-3} \Omega_{\text{osc},3} B_{14} \text{ cm}^{-3}, \quad (11)$$

where Ω_{osc} is the oscillation frequency. Here we assume that the seismic wave is dominated by the base mode which $\Omega_{\text{osc}} \sim (\pi/R)(\mu_s/\rho_n)^{0.5} \sim 10^3$ Hz, where μ_s is the shear modulus and ρ_n the neutron drip density. To generate coherent emissions, charged particles in the bunch would emit with approximately the same phase. Therefore, a comoving volume of the bunch can be estimated as $\eta(\gamma_e c/\nu)^3$. Only fluctuating electron can contribute to the coherent radiation, the number of which is given by

$$\begin{aligned} N_e &= \mu n_e \left(\frac{\gamma_e c}{\nu}\right)^3 \\ &= 9.4 \times 10^{23} \mu \eta_1 \sigma_{s,-3} \Omega_{\text{osc},3} B_{14} \gamma_{e,2}^3 \nu_9^{-3}, \end{aligned} \quad (12)$$

where μ is the fraction of electrons fluctuation and η is the multiplication factors due to the frame transform (Kumar et al. 2017). The total luminosity of the curvature radiation from charged bunches can be described as $L_{\text{iso}} = N_{\text{pat}}(N_e^2 \delta L_{\text{iso}})$, where $\delta L_{\text{iso}} = 2e^2 \gamma_e^8 c / (3\rho^2)$ is the isotropic luminosity in the observer frame, and N_{pat} is the patch number. Thus, we have

$$\begin{aligned} L_{\text{iso}} &= 8.3 \times 10^{39} N_{\text{pat}} \mu^2 \eta_1^2 \sigma_{s,-3}^2 \Omega_{\text{osc},3}^2 \\ &\times B_{14}^2 \gamma_{e,2}^8 \nu_9^{-4} \text{ erg s}^{-1}. \end{aligned} \quad (13)$$

The calculated luminosity is consistent with observations of most repeaters.

The energy release rate during the magnetic reconnection and oscillation-driven activity can both be estimated as

$$\begin{aligned} \dot{E}_R &\simeq 4\pi R_p^2 \delta R \frac{\sigma_s B^2}{8\pi\tau} \\ &= 3.3 \times 10^{42} P_{-3}^{-1} \delta R_4 \sigma_{s,-3} B_{14}^2 \tau_{-3}^{-1} \text{ erg s}^{-1}, \end{aligned} \quad (14)$$

where R_p is the polar cap radius of the remnant star and δR is the height of the crust. The energy release rate for the following starquakes is much smaller than that of the merger stage. Therefore, one expects that there is no any burst detected in the follow-up observation to be as bright as the one triggered by NS-NS merger.

3 PROPERTIES OF FRB 171019

FRB 171019 was originally detected in a wide-field survey of ASKAP (Shannon et al. 2018), hereafter referred to as the ‘‘ASKAP burst.’’ Two weaker repetitions of FRB 171019 were detected in GBT searches on 2018/07/20 and 2019/06/09 (Kumar et al. 2019), hereafter referred to as ‘‘GBT bursts.’’ Another repetition was detected by CHIME on 2019/08/05 (Patek & Chime/Frb Collaboration 2019), hereafter referred to as the ‘‘CHIME burst.’’ Some properties of the bursts are shown in Table 1.

The ASKAP burst is ~ 600 times brighter than the GBT bursts. It is highly possible that the ASKAP burst and the GBT bursts belong to two separate classes of FRBs. In the detailed model calculated in Section 2, we propose that the initial bright burst is generated in a catastrophic event, viz. merger of compact star binary, whereas the two much fainter repetitions are caused by repeating mechanism, viz. starquakes on the merger remnant star.

The the luminosity of a merger-induced burst given by Equation (7) is $\sim 10^3$ times larger than the luminosity of starquake-induced bursts derived in Equation (13). It is noteworthy that this ratio is consistent with the brightness difference between the ASKAP burst and the GBT bursts. In addition, the luminosity of non-repeating bursts given by

Table 1 Properties of FRB 171019 and its Repetitions

No	Telescope	Obs Freq (MHz)	Obs Time (h)	TOA ^d (MJD)	DM (pc · cm ⁻³)	Fluence (Jy · ms)	Burst Width (ms)
1 ^{a,b}	ASKAP	1129.5–1465.5	986.6	58045.56061371	461 ± 1	219 ± 5	5.4 ± 0.3
2 ^b	GBT	720–920	10.6	58319.356770492	456.1 ± 0.4	0.60 ± 0.04	4.0 ± 0.3
3 ^b				58643.321088777	457 ± 1	0.37 ± 0.05	5.2 ± 0.8
4 ^c	CHIME	400–800	17 ± 3	58700.38968	460.4 ± 0.2	≳ 7	6 ± 2

^a Shannon et al. (2018); ^b Kumar et al. (2019); ^c Patek & Chime/Frb Collaboration (2019); ^d Burst time of arrivals are referenced at different frequencies: 1464 MHz for ASKAP, 920 MHz for GBT, and 400 MHz for CHIME.

Equation (7) lies in the more luminous region in Figure 2, while the luminosity of starquake bursts in Equation (13) lies in the less luminous region. The CHIME burst is ~ 10 times brighter than the GBT bursts, which may be explained by an increase of the patch number N_{pat} in our model.

Another noteworthy fact is the non-detection of Parkes follow-up observation. According to Kumar et al. (2019), the Parkes 64-m telescope observed the source for 12.4 hours in total during the 8 month succeeding the ASKAP detection; however, no repeating burst was detected even though the Parkes telescope is much more sensitive than ASKAP. This time length is longer than the timescale given by Equation (8), therefore it is consistent with the timescale of solidification and stress accumulation on the new-born compact star.

However, it is still possible that this luminosity difference derived from observation is caused by the selection effect of observations. Limited by the relatively lower sensitivity, a burst as bright as the GBT bursts or the CHIME burst should be undetectable at ASKAP in fly’s eye mode. Though the GBT and the CHIME observations did not detect bursts as bright as the ASKAP one, it must be taken into consideration that the total observation time at GBT is only 10.6 hours, and only 17 ± 3 hours at CHIME, which are much shorter than the 986.6 hour observation using ASKAP. If so, there could be alternative explanations, such as the bursts are generated by a unified mechanism with a intensity distribution, and the follow-up observations are too short to detect bright ones. In the future, should a repetition burst as bright as FRB 171019 occur, our “merger+starquake” model could be ruled out.

For the binary merger involved in our explanation, it should be an NS-NS or SS-SS merger resulting in a long-lived NS/SS afterwards, rather than a WD-WD or black hole-involved merger. A WD-WD merger would generate a type Ia supernova, however, no optical counterpart of FRBs has been detected. In addition, the supernova remnant would be optically thick for radio emission in a long time after the merger, which is in contradiction with the FRBs detected. As for black hole-involved models, the product would be a black hole, which cannot explain the repeating bursts.

After the NS-NS merger, the mass ejection will shield the following radio emission of the nascent pulsar. Since the optical depth of the relativistic jet launched after the merger decays faster than the slower ejection, and the kilonova ejecta is optically thick in L-band within several decades succeeding the merger (Margalit et al. 2018), the repeating FRBs should be along the relativistic jet, such that one can detect these repeating FRBs under our model. But electrons in the relativistic jet may result in the difference of DM between the one-off FRB and repeating FRBs. The total number of electrons in the relativistic jet can be estimated as

$$N_e \sim \frac{E_{\text{jet}}}{\Gamma m_p c^2} \sim \pi(r\theta)^2 l n_e, \quad (15)$$

where

$$r \sim c\Delta t \quad (16)$$

is the distance from the relativistic jet to source, Δt is time interval between the one-off FRB and repeating FRBs, E_{jet} is total energy of the relativistic jet, n_e is number density of electrons, Γ is saturated bulk Lorentz factor of the relativistic jet, m_p is proton mass, θ is jet opening angle, l is thickness of the relativistic jet. Therefore, the contribution of relativistic jet to DM is

$$\begin{aligned} \text{DM} &= \int_r^{r+l} n_e(r') dr' \sim \frac{E_{\text{jet}}}{\pi \Gamma m_p c^4 \Delta t^2 \theta^2} \\ &= 7.8 \times 10^{-3} E_{\text{jet},50} \Gamma_2^{-1} \theta_{-1}^{-2} \Delta t_7^{-2} \text{ pc} \cdot \text{cm}^{-3}. \end{aligned} \quad (17)$$

It is clear that the effect of relativistic jet on DM is negligible. However, several decades after the merger, the kilonova ejecta would become transparent and contribute $\sim 10^2 \text{ cm}^{-3} \text{ pc}$ to the total DM (Margalit et al. 2018), which may be observable for some sources but not in the case of FRB 171019. It is worth noting that the pulsar of post-merger could be spin down so significantly that its radio luminosity can hardly be detectable on the Earth unless enhanced by starquakes.

4 SUMMARY AND DISCUSSION

Observations show the first brighter burst of FRB 171019 followed by three weaker repeaters about one year later.

In this paper, we propose a unified frame to explain this feature. (i) The first one-off FRB is generated at the moment before NS-NS or SS-SS merger through, e.g., unipolar inductor mechanism. (ii) The nascent remnant SS takes ~ 100 d to be solidified (see Eq. (8)) which accounts for the halcyon period between the one-off burst and the followed repeaters. (iii) After the solidification, starquakes induced by the spin-down of the SS generate the subsequent three weaker repeating FRBs.

Although, the event rate of NS-NS/SS-SS merger seems much smaller than that of FRBs, the jump feature on the luminosities of the first brighter burst of FRB 171019 and the followed repetitions indicates this repeating FRB may belong to a special subclass. In particular, there is probability to directly test our model since the intense one-off burst has a different mechanism from the weak repetitions. For example, one can keep monitoring this source, if another bright burst just like the first one of FRB 171019 were to be detected, then it would mean that our model should be ruled out.

Can a massive NS survive the merger event of binary NSs? This is really a problem that is essentially related to the fundamental strong interaction at low-energy scale and hence to the non-perturbative quantum chromodynamics, the equation of state of cold super-dense matter, which still remains challenging. Nevertheless, it is generally thought that strangeness would play an important role in understanding the state of bulk strong matter (Xu 2018), and pulsars should not be conventional NSs but SSs, formerly called quark cluster star (Xu 2003). The equation of state of strangeon matter would be so stiff that its maximum mass could be as high as $\sim 3 M_{\odot}$ (Lai & Xu 2009), and the later discoveries of $2M_{\odot}$ -pulsars fit the expectation. Furthermore, the merger event of GW 170817 can also be well-understood in the SS model (Lai et al. 2019; Baiotti 2019). Therefore, we anticipate that the unknown equation of state could be the first big problem to be solved in the era of gravitational-wave astronomy.

Acknowledgements The authors thank Dr. Bing Zhang for his valuable discussions. This work is supported by the MoST Grant (2016YFE0100300), the National Key R&D Program of China (2017YFA0402602), NSFC (11633004, 11473044, 11653003, 11673002 and U1531243), the Strategic Priority Research Program of CAS (XDB23010200), and the CAS grants (QYZDJ-SSW-SLH017 and CAS XDB 23040100).

References

Abbott, B. P., Abbott, R., Abbott, T. D., et al. 2017, *ApJ*, 848, L12

- Baiotti, L. 2019, *Progress in Particle and Nuclear Physics*, 109, 103714
- Bannister, K. W., Deller, A. T., Phillips, C., et al. 2019, *Science*, 365, 565
- Chamel, N., & Haensel, P. 2008, *Living Reviews in Relativity*, 11, 10
- Chatterjee, S., Law, C. J., Wharton, R. S., et al. 2017, *Nature*, 541, 58
- Cheng, B., Epstein, R. I., Guyer, R. A., & Young, A. C. 1996, *Nature*, 382, 518
- CHIME/FRB Collaboration, Amiri, M., Bandura, K., et al. 2019a, *Nature*, 566, 235
- CHIME/FRB Collaboration, Andersen, B. C., Bandura, K., et al. 2019b, *ApJ*, 885, L24
- Chruslinska, M., Belczynski, K., Klencki, J., & Benacquista, M. 2018, *MNRAS*, 474, 2937
- Dai, S., Li, L., & Xu, R. 2011, *Science China Physics, Mechanics, and Astronomy*, 54, 1541
- DeLaunay, J. J., Fox, D. B., Murase, K., et al. 2016, *ApJ*, 832, L1
- Duncan, R. C. 1998, *ApJ*, 498, L45
- Goldreich, P., & Julian, W. H. 1969, *ApJ*, 157, 869
- Goldreich, P., & Lynden-Bell, D. 1969, *ApJ*, 156, 59
- Göğüş, E., Woods, P. M., Kouveliotou, C., et al. 1999, *ApJ*, 526, L93
- Hessels, J. W. T., Spitler, L. G., Seymour, A. D., et al. 2019, *ApJ*, 876, L23
- James, C. W. 2019, *MNRAS*, 486, 5934
- Jin, Z.-P., Li, X., Wang, H., et al. 2018, *ApJ*, 857, 128
- Kashiyama, K., Ioka, K., & Mészáros, P. 2013, *ApJ*, 776, L39
- Katz, J. I. 2014, *Phys. Rev. D*, 89, 103009
- Keane, E. F., Stappers, B. W., Kramer, M., & Lyne, A. G. 2012, *MNRAS*, 425, L71
- Kulkarni, S. R., Ofek, E. O., Neill, J. D., Zheng, Z., & Juric, M. 2014, *ApJ*, 797, 70
- Kumar, P., Lu, W., & Bhattacharya, M. 2017, *MNRAS*, 468, 2726
- Kumar, P., Shannon, R. M., Osłowski, S., et al. 2019, arXiv e-prints, arXiv:1908.10026
- Lai, X. Y., & Xu, R. X. 2009, *MNRAS*, 398, L31
- Lai, X., Zhou, E., & Xu, R. 2019, *European Physical Journal A*, 55, 60
- Lin, M.-X., Xu, R.-X., & Zhang, B. 2015, *ApJ*, 799, 152
- Liu, X. 2018, *Ap&SS*, 363, 242
- Lorimer, D. R., Bailes, M., McLaughlin, M. A., Narkevic, D. J., & Crawford, F. 2007, *Science*, 318, 777
- Luo, R., Lee, K., Lorimer, D. R., & Zhang, B. 2018, *MNRAS*, 481, 2320
- Luo, R., Men, Y., Lee, K., et al. 2020, arXiv e-prints, arXiv:2003.04848
- Marcote, B., Paragi, Z., Hessels, J. W. T., et al. 2017, *ApJ*, 834, L8

- Margalit, B., Metzger, B. D., Berger, E., et al. 2018, *MNRAS*, 481, 2407
- Michilli, D., Seymour, A., Hessels, J. W. T., et al. 2018, *Nature*, 553, 182
- Murase, K., Mészáros, P., & Fox, D. B. 2017, *ApJ*, 836, L6
- Oppermann, N., Yu, H.-R., & Pen, U.-L. 2018, *MNRAS*, 475, 5109
- Palenzuela, C., Lehner, L., Liebling, S. L., et al. 2013, *Phys. Rev. D*, 88, 043011
- Patek, C., & Chime/Frb Collaboration. 2019, *The Astronomer’s Telegram*, 13013, 1
- Paul, D. 2018, *MNRAS*, 477, 4275
- Peters, P. C. 1964, *Physical Review*, 136, 1224
- Petroff, E., Johnston, S., Keane, E. F., et al. 2015, *MNRAS*, 454, 457
- Petroff, E., Barr, E. D., Jameson, A., et al. 2016, *PASA*, 33, e045
- Pol, N., McLaughlin, M., & Lorimer, D. R. 2019, *ApJ*, 870, 71
- Ponce, M., Palenzuela, C., Lehner, L., & Liebling, S. L. 2014, *Phys. Rev. D*, 90, 044007
- Pons, J. A., Reddy, S., Prakash, M., Lattimer, J. M., & Miralles, J. A. 1999, *ApJ*, 513, 780
- Shannon, R. M., Macquart, J. P., Bannister, K. W., et al. 2018, *Nature*, 562, 386
- Spitler, L. G., Scholz, P., Hessels, J. W. T., et al. 2016, *Nature*, 531, 202
- Suvorov, A. G., & Kokkotas, K. D. 2019, *MNRAS*, 488, 5887
- Tendulkar, S. P., Bassa, C. G., Cordes, J. M., et al. 2017, *ApJ*, 834, L7
- Thompson, C., Lyutikov, M., & Kulkarni, S. R. 2002, *ApJ*, 574, 332
- Thornton, D., Stappers, B., Bailes, M., et al. 2013, *Science*, 341, 53
- Totani, T. 2013, *PASJ*, 65, L12
- Wadiasingh, Z., & Timokhin, A. 2019, *ApJ*, 879, 4
- Wang, J.-S., Yang, Y.-P., Wu, X.-F., Dai, Z.-G., & Wang, F.-Y. 2016, *ApJ*, 822, L7
- Wang, J.-S., Peng, F.-K., Wu, K., & Dai, Z.-G. 2018a, *ApJ*, 868, 19
- Wang, W., Luo, R., Yue, H., et al. 2018b, *ApJ*, 852, 140
- Wang, W., Zhang, B., Chen, X., & Xu, R. 2019, *ApJ*, 876, L15
- Xu, R. 2018, *Science China Physics, Mechanics, and Astronomy*, 61, 109531
- Xu, R. X. 2003, *ApJ*, 596, L59
- Yamasaki, S., Totani, T., & Kiuchi, K. 2018, *PASJ*, 70, 39
- Yang, Y.-P., & Zhang, B. 2018, *ApJ*, 868, 31
- Yu, M., & Xu, R. X. 2011, *Astroparticle Physics*, 34, 493
- Yuan, M., Lu, J.-G., Yang, Z.-L., Lai, X.-Y., & Xu, R.-X. 2017, *RAA (Research in Astronomy and Astrophysics)*, 17, 092